Biomaterials Science

ROYAL SOCIETY OF CHEMISTRY

PAPER

View Article Online
View Journal | View Issue

Cite this: *Biomater. Sci.*, 2023, **11**, 6919

Biomechanical characterization of a fibrinogen–blood hydrogel for human dental pulp regeneration

Sofia Silvia Piglionico, *[a,b] Bela Varga,[c] Orsolya Pall,[a] Olivier Romieu,[a] Csilla Gergely,[c] Frédéric Cuisinier,[a] Bernard Levallois[a] and Ivan Vladislavov Panayotov[a]

In dental practice, Regenerative Endodontic Treatment (RET) is applied as an alternative to classical endodontic treatments of immature necrotic teeth. This procedure, also known as dental pulp revitalization, relies on the formation of a blood clot inside the root canal leading to the formation of a reparative vascularized tissue similar to dental pulp, which would provide vitality to the affected tooth. Despite the benefit of this technique, it lacks reproducibility due to the fast degradation and poor mechanical properties of blood clots. This work presents a method for constructing a fibrinogen–blood hydrogel that mimics the viscoelastic properties of human dental pulp while preserving the biological properties of blood for application in RET. By varying the blood and fibrinogen concentrations, gels with different biomechanical and biological properties were obtained. Rheology and atomic force microscopy (AFM) were combined to study the viscoelastic properties. AFM was used to evaluate the elasticity of human dental pulp. The degradation and swelling rates were assessed by measuring weight changes. The biomimetic properties of the gels were demonstrated by studying the cell survival and proliferation of dental pulp cells (DPCs) for 14 days. The formation of an extracellular matrix (ECM) was assessed by multiphoton microscopy (MPM). The angiogenic potential was evaluated by an *ex vivo* aortic ring assay, in which the endothelial cells were observed by histological staining after migration. The results show that the Fbg–blood gel prepared with 9 mg ml^{-1} fibrinogen and 50% blood of the Fbg solution volume has similar elasticity to human dental pulp and adequate degradation and swelling rates. It also allows cell survival and ECM secretion and enhances endothelial cell migration and formation of neovessel-like structures.

Received 24th March 2023,
Accepted 17th August 2023

DOI: 10.1039/d3bm00515a

rsc.li/biomaterials-science

1. Introduction

Dental pulp is the soft tissue responsible for tooth vitality situated in canals inside the root of a tooth. Caries or tooth trauma could damage dental pulp, which becomes necrotic. In these cases, classical endodontic treatments could be performed to remove the damaged tissue and disinfect and seal the canal with an inert material to allow permanence of the non-vital tooth in the mouth.

However, in young patients whose teeth are still immature and root formation has not been completed, treatment and prognosis become complicated, frequently resulting in inevitable tooth loss. In these cases, regenerative endodontic procedures could be applied as an alternative to classical endodontic treatments.

The objective of this treatment is to obtain a reparative vascularized and innervated tissue with an architecture similar to dental pulp, which would provide vitality to the affected tooth and allow continuity in root development.[1] This procedure relies on evoked periapical bleeding followed by blood clot formation inside the root canal which will ensure periapical healing and apical closure.[2,3] This blood clot would act as a scaffold containing growth factors and undifferentiated cells coming from the periapical zone by cell homing.[4,5] Despite the potential benefit of revascularization treatment, dentists faced problems of not only a lack of predictability and stability of these techniques due to incomplete disinfection and variability in blood quantity and component concentration between patients, but also a fast degradation rate and poor mechanical properties of the blood clot.[6,7] These factors have led to efforts to search for more effective scaffolds such as synthetic or natural polymers.[8]

[a]*LBN, Univ Montpellier, Montpellier, France. E-mail: sofiapiglionico@hotmail.com, pallorsi90@gmail.com, olivier.romieu@umontpellier.fr, frederic.cuisinier@umontpellier.fr, bernard.levallois@umontpellier.fr, ivan.panayotov@umontpellier.fr*
[b]*Centro de Investigaciones Odontológicas, National University of Cuyo, Argentina*
[c]*L2C, Univ Montpellier, CNRS, Montpellier, France. E-mail: csilla.gergely@umontpellier.fr, beduska@gmail.com*

From a biological point of view, a suitable scaffold for dental pulp regeneration purposes should mechanically mimic the dental pulp tissue, support cell survival, migration, and differentiation for optimal tissue regeneration, and have a degradation rate in accordance with the extracellular matrix secretion rate.[9] Given the biologically favorable properties of the intracanal blood clot, approaches for improving its reliability may secure this scaffold for Regenerative Endodontic Treatment (RET).[10] In order to take advantage of these properties, autologous blood-derived products such as PRP (platelet-rich plasma) and PRF (platelet-rich fibrin) have been used for dental pulp regeneration. However, PRP and PRF fail to demonstrate a significant advantage over an induced blood clot in RET.[11] The main difference of these products from whole blood is the presence of red blood cells (RBC) and leukocytes. These cells are reservoirs of cytokines[12] and have the potential to participate in the inflammatory response and in tissue repair since they could interact with the main components of ECM, such as collagen and fibronectin, and display cytokine interactions.[13]

Another key factor for blood clotting is fibrin. During the process of coagulation, fibrinogen is cleaved by thrombin and polymerizes to form a fibrin network. Fibrin provides consistency to the blood clot, forming a natural, biocompatible, and biodegradable polymeric network that allows cell survival and enhances cell interactions *via* integrin or non-integrin receptors.[14–16] Different authors have already described the use of purified fibrin as an injectable scaffold for several medical applications.[17,18] Purified fibrin has also been tested for RET purposes *in vivo* showing beneficial results such as neovessel formation.[19] However, the poor mechanical strength and rapid degradation rate of fibrin set limits on its clinical applications.[20] A strategy to enhance the mechanical and biological characteristics of the fibrin network could be the modification of the concentration of blood components, such as fibrinogen. This has already been proposed and applied in the neural regeneration field.[21]

This study presents the development of an injectable fibrinogen–blood hydrogel for Regenerative Endodontic Treatment. The gel is made of purified fibrinogen (Fbg) mixed with human blood. By using blood, cells and growth factors beneficial for tissue regeneration are preserved. By increasing the fibrinogen concentration in the blood clot, gel elasticity and biodegradability could be successfully modulated, leading to a promising biomaterial that could mimic human dental pulp.

2. Materials and methods

2.1. Blood collection

Human blood was obtained from the cubital vein of healthy volunteers in tubes containing 0.109 M sodium citrate (9NC, BD Vacutainer). All blood samples were collected at the French Establishment of Blood in accordance with the French Public Health Code, Titles I and II of the book, law number 98-535 of July 1, 1998 on the reinforcement of health monitoring and control of the safety of products intended for human use; law number 2004-800 of August 6, 2004 relating to bioethics; and Decision of November 6, 2006 defining the principles of good practice provided for in Article L.1223-3 of the French Public Health Code. After obtaining the informed consent of the patients, blood products were randomly provided to the University of Montpellier for this project under commitment no. 21PLER2021-027. Citrated blood was refrigerated at 4 °C and used within 24 hours of collection.

2.2. Gel preparation

The fibrinogen–blood gel was obtained by mixing a fibrinogen (Fbg) solution with human blood and calcium chloride ($CaCl_2$) to reverse the effect of sodium citrate and reactivate the coagulation process.

The fibrinogen solution was obtained from lyophilized bovine fibrinogen powder (Sigma-Aldrich, USA) diluted in DMEM (Gibco, Life Technologies Limited, UK) at different concentrations (3, 6, 9, 12 mg ml^{-1}). The blood content was calculated as a ratio of the Fbg solution volume and quantified as a percentage. For example, a final preparation of gel containing blood at 50% of the Fbg solution volume contains 1 part of fibrinogen solution, $\frac{1}{2}$ part of blood, and $\frac{1}{4}$ part of $CaCl_2$.

2.3. Rheological measurements

a. Study groups. For rheological measurement, two groups of Fbg–blood-containing hydrogels were studied and are summarized in Table 1. The experiment was conducted in two groups. In the first group, the blood content was changed to 40%, 50%, 60%, 70%, and 80% of the Fbg solution volume while maintaining a constant fibrinogen concentration of 3 mg ml^{-1}. In the second group, the Fbg concentration was varied between 3 mg ml^{-1}, 6 mg ml^{-1}, and 9 mg ml^{-1} while keeping the blood content constant at 50% of the Fbg solution volume. All experimental groups were studied in triplicate.

b. Rheology. Samples from group 2 were evaluated by Small Amplitude Oscillatory Shear (SAOS) techniques using a rheometer (Anton Paar MCR 502, Germany). A small amount of the sample (690 μL–0.99 mm gap) was placed between a cone and a disc immediately after preparation in a liquid state before gelation occurred. First, an amplitude sweep at 20 °C up to 5% strain was conducted to measure the frequency ranges of the Linear Viscoelastic Region (LVR). To describe the viscoelastic behavior of the gel, frequency sweeps were performed to determine the storage modulus G' (elastic behavior) and the loss shear modulus G'' (viscous behavior). 5% strain

Table 1 Experimental groups for study of mechanical properties of the Fbg–blood-containing gel

Group 1	Group 2
Blood concentration varied (40–50–60–70–80% of Fbg solution volume)	Blood concentration constant (50% of the Fbg solution volume)
Fbg concentration constant (3 mg ml^{-1})	Fbg concentration varied (3, 6, 9 mg ml^{-1})

was applied, in a range from 0.628 to 628 rad per s (from 0.1 to 100 Hz) at 121 points, after 10 and 30 minutes of gel preparation, at 20 °C and 37° C.

c. Inertia corrections. Frequency sweep curves at high frequencies present a slope of around the square of ω (angular velocity), and this indicates that inertia dominates the frequency sweep curves at high frequencies.[22] This is the reason why instrument inertia contributions were corrected for G' values using the equation $G's = G' + I\omega^2K_g$,[23] where $G's$ are the values of G' without inertia contributions, I is inertia equivalent to the torque ratio of the material, ω corresponds to the angular velocity and K_g is the geometry factor of η (loss factor). The sample storage modulus $G's$ is the sum of the real part of the measured modulus and an inertia correction term, which increases with the square of the test frequency. Values of the loss modulus G'' were not corrected.

2.4. Elasticity measurements of the natural pulp tissue and Fbg–blood gel

a. Dental pulp tissue isolation for AFM. Dental pulp elasticity was measured for comparison with Fbg–blood gel elasticity. Dental pulp was obtained from freshly extracted premolar teeth collected from the dental medical center of Montpellier Hospital. To extract the dental pulp tissue, a groove was made at the cementum–enamel junction with a diamond disc to carefully separate the crown from the root, without pulp sectioning. The dental pulp tissue was carefully taken out with forceps and divided into two with a scalpel: coronal and root pulp. Both parts were adhered to the surface of a small Petri dish with Cell-Tak (Corning, NY) and kept overnight in DMEM at 37 °C under 5% CO_2 before measurements. Pulp tissues from 3 extracted premolar teeth were used for this experiment.

b. Elastic modulus measurements by AFM. Measurements of gel elasticity were performed 30 minutes after gel polymerization at 37 °C for both groups 1 and 2. All AFM measurements were performed under liquid conditions (in DPBS, Hyclone GE Healthcare Life, Utah) at room temperature with an MFP-3D head coupled to the Molecular Force Probe 3D controller (Asylum Research, Santa Barbara, CA). Force-indentation profiles of the Fbg–blood-containing gel were collected using a 10 nN trigger force applied using sQube Gold sphere colloidal cantilevers with a radius of 3–5.5 mm and a nominal spring constant of 32 pN nm^{-1} (CP-PNPL-Au-B5, NanoAndMore GmbH, Germany). Five different zones were chosen for each gel sample and 8 zones were chosen for coronal and root natural pulp tissues, respectively. Force maps of 10 × 10 pixels (4 μm each pixel) were acquired on 40 × 40 μm^2 surface areas. Cantilever spring constants were determined before every measurement using the thermal noise method available in the Asylum Research software.[24] Young's modulus (E) was calculated from the approaching part of the curve, using a modified Hertz model developed for different AFM tip shapes.[25] Poisson's ratio of the cells was assumed to be 0.5, as suggested for incompressible materials.[26]

2.5. Degradation and swelling rate measurements

To assess the permeability and dimensional stability of the Fbg–blood gel, both swelling rate and degradation rate were measured. Two study groups of Fbg–blood gels were evaluated by measuring their weight changes in PBS (pH 7.4) at 37 °C, following a previously described protocol.[27] The first group had varying Fbg concentrations (3, 6, and 9 mg ml^{-1}) and a constant blood concentration (50% of the Fbg solution volume). The second group had a constant Fbg concentration (9 mg ml^{-1}), with varying blood concentrations (50% and 80% of the Fbg solution volume). The samples were prepared in triplicate, molded, and incubated in a 24-well plate at 37 °C for 1 h to allow gelation. The samples were weighed (W_0) after being taken out from their molds; then they were placed in small Petri dishes and immersed in PBS and their weight changes (W_t) were measured to evaluate degradation over 14 days. Pictures were taken on days 0, 4, 10, and 14. The percentages of degradation and swelling were calculated as follows:

$$\text{Degradation } \% = [(W_0 - W_t)/W_0] \times 100.$$

$$\text{Swelling } \% = [(W_t - W_0)/W_0] \times 100.$$

W_0 and W_t are the weights of the hydrogels before and after soaking in PBS, respectively.

2.6. Human dental pulp cell proliferation in the Fbg–blood hydrogel

a. Isolation of primary dental pulp cells. Primary dental pulp cells were recovered from extracted third molars following a previously described protocol.[28] Briefly, the pulp was carefully taken out with forceps and a K-file no. 25 and digested for 1 hour at 37 °C in a solution of 3 mg ml^{-1} collagenase and 4 mg ml^{-1} dispase (BD Biosciences, Bedford, MA). After filtration through a 70 Falcon strainer, the solution was mixed with αMEM (Gibco, Life Technologies Limited, UK) supplemented with 10% fetal bovine serum, 100 U ml^{-1} penicillin, and 100 μg mL^{-1} streptomycin (Invitrogen, Carlsbad, CA, USA). The medium was changed 24 hours after cell seeding to remove non-adherent cells. Cells were incubated in cell-adherent culture flasks until 80% confluency and placed to proliferate in an incubator at 37 °C under 5% CO_2.

b. Gel for DPC proliferation. The Fbg–blood-containing hydrogel was prepared as described above with different concentrations of Fbg (3, 6, 9, 12 mg ml^{-1}) and blood equal to 50% of the final Fbg solution volume. A concentration of 175,000 cells per ml of the final volume of Fbg–blood gel solution was added before mixing it with blood. The samples were prepared in triplicate in a 48-well plate. All samples were maintained in αMEM + 1%PS + 5%SVF at 37 °C under 5% CO_2.

c. Epi-fluorescence microscopy. To track dental pulp cells (DPCs) inside the gel, the cells were transfected by a retrovirus encoding the Red Fluorescent Protein (RFP) and expanded. To an 80% confluent flask with 10 ml αMEM was added 100 ml of lentivirus and 8 μl of sure entry (SureENTRY™ Transduction Reagent, QIAGEN, Germany) previously diluted in PBS (5 μl ml^{-1}). Due to the reporter gene on the lentiviral construct,

their fluorescence could be easily detected at 625–740 nm wavelength (red).

Epi-fluorescence microscopy was performed with an Eclipse TE2000-E (Nikon) microscope. After 3, 7 and 14 days, the samples of the Fbg–blood-containing gel containing RFP–DPC were fixed in 4% paraformaldehyde for 24 hours and then washed with PBS and observed using CFI Plan Fluor 10_/0.3 (Nikon) objectives and a Y-2E/C filter (540–580 nm; dichromatic mirror (DM): 595 nm, barrier filter (BA): 600–660 nm; Nikon). The recorded microscopy images of the gel surfaces were used to count the cells present inside them.

d. Cell counting. Multiple images were captured to analyze the entire surface of the gels at 10× magnification and processed using ImageJ (Fiji version 1.48 April 2014).[29] They were converted into 8-bit images to render them binary and the gel surface area revealing pixels corresponding to RFP–DPC was automatically quantified using the particle analysis tool.

2.7. Structural organization of the Fbg–blood gel during DPC proliferation

a. Multiphoton microscopy. The structural extracellular matrix organization of the Fbg–blood hydrogel was assessed by multiphoton microscopy (MPM). Dental pulp cells (175,000 cells per ml) were added to the Fbg–blood-containing hydrogel (9 mg ml^{-1} fibrinogen and 50% blood of the final Fbg solution volume). The gel's structure was analyzed 3 days, 14 days, and 21 days after incubation in the cell culture medium αMEM (Gibco, Life Technologies Limited, UK) supplemented with 10% fetal bovine serum, 100 U ml^{-1} penicillin, and 100 μg mL^{-1} streptomycin (Invitrogen, Carlsbad, CA, USA) at 37 °C. All samples were prepared in triplicate. Histological slices with a thickness of 3 μm were obtained from each gel.

Images were captured using a custom-built multiphoton microscope based on a Zeiss Imager Z1 upright microscope (Zeiss, Jena, Germany). A 450 nm low-pass filter was used and MPM images were reconstructed using point-by-point scanning based on the non-linear emission spectra from each pixel.[30] The two-photon fluorescence (2-PEF) signal was used to detect blood cells and autofluorescent structures in the gel. A second harmonic generation signal (SHG) was used to image collagen structures. The recovered images were processed using ImageJ software (Fiji version 1.48 April 2014).[29] Autofluorescence is indicated in green.

2.8. *Ex vivo* rat aortic ring assay

a. Aortic ring isolation. To evaluate endothelial cell migration and assess neo-vessel formation inside the Fbg–blood gel, an *ex vivo* rat aortic ring assay was performed at different compositions of the gel. Aortas from adult rats that were euthanized for other reasons, without systemic conditions, were collected following a protocol already described.[31] Briefly, immediately after death, the thoracic aorta was carefully dissected and washed with OptiMEM (Gibco, Life Technologies Limited, UK). After the removal of the surrounding fatty tissue, rings of about 1 mm thickness were cut with a scalpel and incubated overnight in OptiMEM at 37 °C under 5% CO_2. One aortic ring was placed in each well of a 24-well plate and covered with 500 μl of Fbg–blood gel prepared at different concentrations of Fbg (3, 6, 9, and 12 mg ml^{-1}). The volume of blood was kept constant for all preparations at 50% of the Fbg solution volume (blood content = 50% of the Fbg volume solution). A fibrin solution containing 3 mg ml^{-1} Fbg, without blood, was used as the negative control. All samples were maintained in αMEM + 1%PS + 5% SVF at 37 °C under 5% CO_2 for 10 days.

b. Histology. After fixation of the samples, they were treated in an impregnation automaton Leica ASP300 and embedded in paraffin with an MYR EC350 paraffin embedding station. Paraffin blocks were cut at a thickness of 3 μm using a Microm HM340E microtome equipped with a Niagara system and placed on coated glass slides (Superfrost). Hematoxylin–eosin staining was performed on the slices. Images were captured at 5× magnification. After converting them into binary images using ImageJ (Fiji version 1.48 April 2014), the aorta area was extracted, and the surface area covered by pixels corresponding to endothelial cells was quantified. The spreading index (the inverse of cell circularity) was calculated (4pi (area/perimeter^2)); a value of 0 indicates a perfect circle (red blood cells) and a value of 1 indicates an increasingly elongated shape (endothelial cells).

2.9. Statistical analysis

The collected data were processed using SigmaPlot 11.0 (Systat Software, Inc, 2008) to calculate mean and standard deviation values. As all data passed the normality test (Shapiro–Wilk method) and equal variance tests (*F*-test), parametric statistics were used to compare the groups. The data were analyzed using a one-way Analysis of Variance (ANOVA) with a significant variance of ($p \leq 0.05$). All pairwise multiple comparison procedures (Holm–Sidak method) were conducted with an overall significance level of 0.05.

3. Results

3.1. Rheological measurements of the Fbg–blood-containing hydrogel

The viscoelastic behavior of a material can be determined through rheological measurements by calculating the storage modulus G' and the loss shear modulus G''. Viscoelastic behavior of gels is characterized by a Linear Viscoelastic Regime (LVR) indicating a linear relationship between G' and G'' through frequency. Fig. 1 shows the logarithmic variation of G' and G'' through frequencies for three different concentrations of Fbg in tested hydrogels: 3 mg ml^{-1} (green curve), 6 mg ml^{-1} (blue curve), and 9 mg ml^{-1} (red curve). Two time points of jellification (after 10 min and 30 min) at two different temperatures (20 °C and 37 °C) were tested.

Corrected values of G' at 20 °C after 10 minutes of jellification are around 20.21 Pa for 3 mg ml^{-1}; 36.54 Pa for 6 mg ml^{-1} and 53.33 Pa for 9 mg ml^{-1} Fbg. After 30 minutes, G' values increase for all preparations: for 3 mg ml^{-1} Fbg, it is around

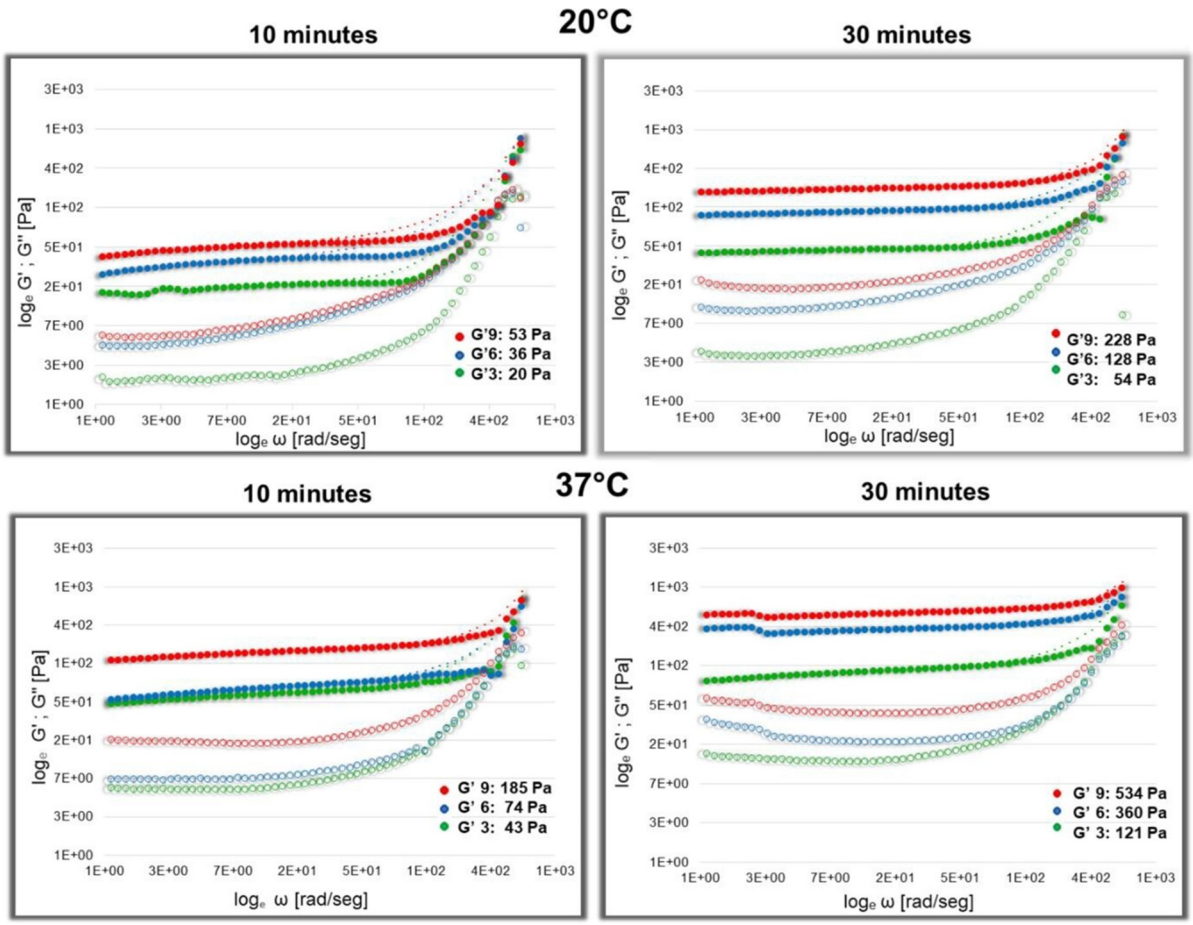

Fig. 1 Rheological measurements of different preparations of gel. The logarithmic dependence of *G*′ and *G*″ values on frequency for three different concentrations of Fbg in the Fbg–blood gel: 3 mg ml^{-1} (green), 6 mg ml^{-1} (blue), and 9 mg ml^{-1} (red), after 10 and 30 minutes of jellification time and at two different temperatures: 20 °C and 37 °C. Inertia-corrected *G*′ values are indicated by full dots, and *G*′ values without correction of inertia are indicated by small dots. *G*″ values are represented by empty circles.

53.95 Pa; for 6 mg ml^{-1} Fbg, 128.44 Pa and for 9 mg ml^{-1} Fbg, 228.16 Pa. The elasticity of the gel increases notably at 37 °C. Ten minutes after preparation, *G*′ is 43.19 Pa for the lowest Fbg concentration, 74.52 Pa for 6 mg ml^{-1} Fbg and 185.58 Pa for preparations with 9 mg ml^{-1} Fbg. Within 30 minutes, values of *G*′ are higher: they vary around 121.69 Pa, 360.63 Pa, and 534.92 Pa for 3, 6, and 9 mg ml^{-1}, respectively. Furthermore, the elasticity of the gel is more stable at 37 °C since LVR shows less variability at high frequencies.

3.2. Elasticity measurements of the natural pulp tissue and Fbg–blood hydrogel

The elastic properties of the gels were compared with the elasticity of human dental pulp from freshly extracted premolars *via* AFM nanoindentation measurements.

In experimental group number one (see Materials and methods), where the blood content in the gel was increased (with a constant Fbg concentration: 3 mg ml^{-1}), the Young modulus of the gels increased (Fig. 2A): from 132.75 Pa (for 40% blood) to 681 Pa (for 80% blood). The increment is statistically significant after a 60% blood concentration ($p <$ 0.001). Measurements demonstrated that the gel with elastic properties similar to the human dental pulp could be obtained by changes in Fbg and/or blood concentration in the gel.

In experimental group number two, with variable Fbg concentrations, the Young modulus of the gels increased significantly ($p \leq 0.001$) for a higher (9 mg ml^{-1}) Fbg concentration (Fig. 2B). The Young modulus values measured by AFM in Fbg–blood-containing gels are as follows: 143.5 Pa for 3 mg ml^{-1} Fbg; 334.5 Pa for 6 mg ml^{-1} Fbg and 517.836 Pa for 9 mg ml^{-1} Fbg. These values are similar to those obtained in the rheological study under the same conditions (at 37 °C, 30 min after preparation). The measured mean of dental pulp Young modulus for coronal pulp is 419 Pa and 672 Pa for root pulp. These values present no statistically significant difference from those obtained for Fbg–blood-containing gels prepared with an Fbg concentration of 9 mg ml^{-1}.

3.3. Degradation and swelling rate measurements

The swelling and degradation rates of Fbg–blood gels over 14 days are presented in Fig. 3. During the first seven days, swelling takes place with a more stable variation in Fbg–blood gels

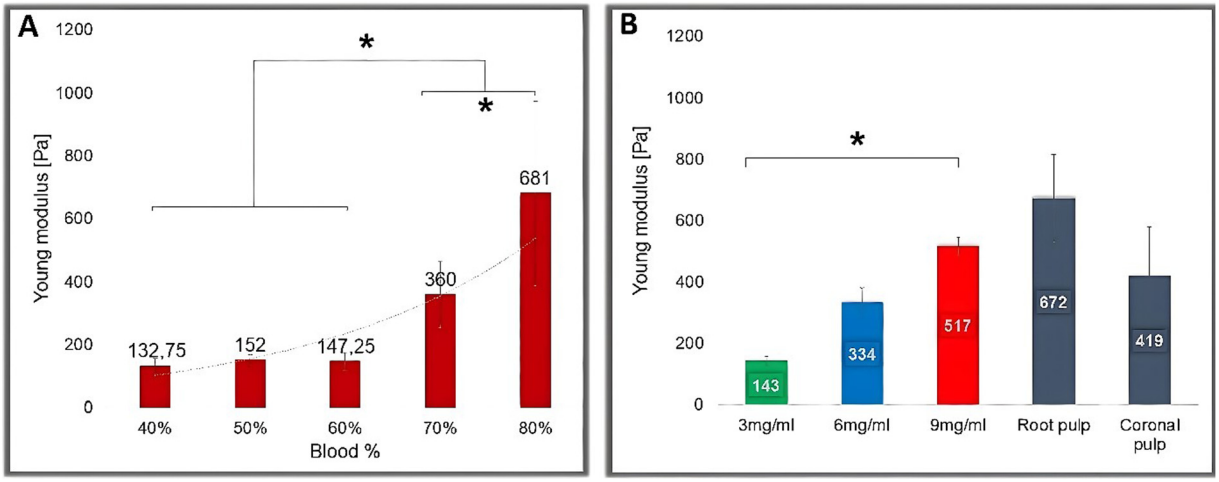

Fig. 2 AFM measurements of elastic properties of the Fbg–blood gel and human dental pulp. (A) Young moduli measured on the Fbg–blood gel with different blood concentrations. The Fbg concentration in all groups is 3 mg ml^{-1}. Elasticity increases while increasing blood concentrations. The difference is significant ($p \leq 0.001$) between 70% and 80% blood *vs.* 40%, 50% and 60% blood concentrations. (B) Young moduli measured on dental pulp and the Fbg–blood gel with different Fbg concentrations. Elasticity values increase significantly while increasing Fbg content ($p \leq 0.001$). Young moduli obtained with 9 mg ml^{-1} Fbg present no statistically significant difference compared to the elasticity values of human dental pulp.

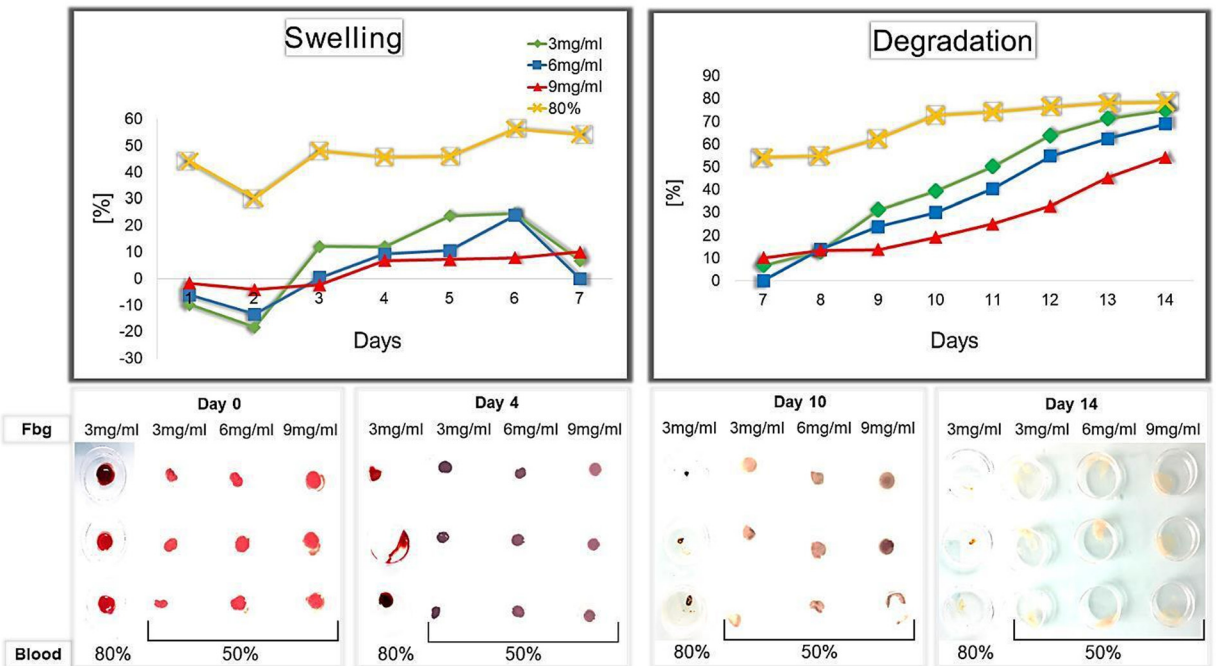

Fig. 3 Swelling and degradation rates of the Fbg–blood-containing gel with different Fbg and blood concentrations. Pictures of gels with concentrations and at different times (days 0, 4, 10, and 14).

prepared at a higher fibrinogen concentration (9 mg ml^{-1}). The maximum point of swelling is reached after 6 days for all concentrations of Fbg: 24.52% for 3 mg ml^{-1}; 23.83% for 6 mg ml^{-1}; 7.76% for 9 mg ml^{-1} with statistically significant difference ($p \leq 0.001$) for the gel with 9 mg ml^{-1} Fbg. For Fbg–blood-containing gels with a blood concentration of 80% and 3 mg ml^{-1} Fbg, the highest point of swelling is also observed on day 6 (56.18%). This point is significantly higher than the groups made with 50% blood ($p = 0.001$).

The degradation of all Fbg–blood gels starts after 7 days of incubation, and the calculated degradation rates increase with time for all Fbg concentrations. The progression of degradation is faster and more accentuated at lower concentrations of Fbg (the slope is 10.72 per day for 3 mg ml^{-1}, 9.39 for 6 mg

ml^{-1}, and 5.83 for 9 mg ml^{-1}); this difference is statistically significant for the 9 mg ml^{-1} Fbg gel. After 14 days the degradation rate reaches 80.32% for clots made of 80% blood. For blood clots made with 50% blood, the degradation rate is lower for all Fbg concentrations: 74.78% for 3 mg ml^{-1}, 68.72% for 6 mg ml^{-1}, and 54.16% for 9 mg ml^{-1}, indicating that the Fbg gel with 9 mg ml^{-1} Fbg is the most stable.

3.4. Cell proliferation of human dental pulp cells in the Fbg–blood hydrogel

Cell survival and proliferation were assessed by fluorescence microscopy images of gels obtained with various fibrinogen concentrations (3, 6, 9, 12 mg ml^{-1}) after three incubation times (3, 7, and 14 days) (Fig. 4B and C). The results show that after 3 days, DPC proliferation is significantly higher for 9 mg ml^{-1} (p = 0.003) and 12 mg ml^{-1} (p = 0.001) compared to 3 mg ml^{-1} Fbg. After 7 days, the gel with 3 mg ml^{-1} Fbg was completely degraded and the gel with 6 mg ml^{-1} Fbg was highly degraded. As a consequence, the number of living cells in these gels is exceptionally low.

Cell proliferation in the 9 mg ml^{-1} Fbg gel is higher with a statistically significant difference ($p \leq 0.001$) compared to all other gels after 7 days of incubation (Fig. 4C). After 14 days, the number of DPCs in the gel decreases and the proliferation rates for 9 mg ml^{-1} and 12 mg ml^{-1} are practically equal. At the end of the proliferation period, a specific cell organization of DPCs in fiber-like conglomerates was observed under both conditions.

3.5. Structural organization of the Fbg–blood hydrogel during DPC proliferation

Multiphoton microscopy images of Fbg–blood-containing gels prepared with 9 mg ml^{-1} Fbg were obtained to assess the evolution of fibrin network over time. After 3 days, red blood cells (RBC) and DPCs present in the gel showed autofluorescence. However, at this stage, the fibrin network was not revealed by 2-PEF. After 2 weeks, the structure changed, RBCs were less abundant, and an auto-fluorescent network appeared. At 3 weeks, this network seemed more organized and denser fibers are present on it. Nevertheless, no second harmonic generation signal suggesting collagen type I formation was detected (Fig. 4A).

3.6. *Ex vivo* rat aortic ring assay

The rat aortic ring assay was used to evaluate endothelial cell migration from aorta rings placed inside Fbg–blood gels that do not contain dental pulp cells. Gels were prepared with different concentrations of Fbg (3, 6, 9 and 12 mg ml^{-1}) and constant blood concentration for all preparations (final blood volume = 50% of the Fbg solution volume). Analysis of histological slices demonstrated that the endothelial cell migration is different when the Fbg concentration was changed (the histogram shown in Fig. 5). A significantly higher area of cell migration within the Fbg–blood-containing gel was found only with 9 mg ml^{-1} Fbg compared to the fibrin control group, whereas in the Fbg gel with 12 mg ml^{-1} Fbg, the cell migration area appeared to decrease. In terms of the blood vessel formation, the histological images presented in Fig. 5 reveal the characteristic organization of tubule-like structures (red arrows) formed by endothelial cells.

4. Discussion

Following the principle of mechanotransduction, mechanical signals such as elasticity coming from the scaffold should be similar to those of the tissue that want to be replaced because they will be transduced into chemical signals to the cell nucleus, affecting RNA expression, leading to cell proliferation and differentiation similar to the surrounding tissue.[32,33] This is the reason why biomaterials used for RET should mechanically mimic human dental pulp.

In this study, a Fbg–blood gel for RET with elasticity similar to the dental pulp is proposed. The accuracy of AFM measurements allows the determination of the mean coronal pulp elasticity at 419 Pa (±159) and root pulp at 672 Pa (±142). These values differ from those found by rheological measurements by Erisken *et al.*, who reported around 100 Pa but in porcine pulp.[34] However, pulp elasticity values showed a good correlation with those obtained with 9 mg ml^{-1} Fbg and 50% blood in the gel (531 Pa). These values do not exhibit statistically differences from those of human dental pulp.

The Young's modulus increases with a higher concentration of Fbg and also with a larger portion of blood within the gel. This increase could be due to the higher presence of red blood cells (RBCs), as the fracture strain of a clot depends on the volume of RBCs.[35] Gersh *et al.* have confirmed that RBCs play a role in shaping the fibrin network, with the highest Young's modulus achieved when 10% RBCs were added to purified fibrin networks. This modulus gradually declines until 50% RBCs with clot alteration.[36] Since whole blood contains around 38% RBCs, an Fbg–blood gel prepared with 80% blood should contain 10.8–11.9% RBCs in its structure. To maintain clot integrity and avoid the peak of 10% RBCs, a preferred concentration of 50% blood is recommended for Fbg–blood gel preparation.

The gel elasticity obtained by AFM was confirmed by rheological measurements, which allows a detailed analysis of the viscoelastic behavior. The gel displayed specific behaviors typical of gels due to its viscoelastic nature, combining aspects of both liquids and solids in its response to external forces, since values of G' are higher and parallel to G''. However, they increase at high frequencies, mostly in inertia uncorrected values of the storage modulus G'. Subsequently, after inertia correction of G', the Linear Viscoelastic Regime (LVR) is less dependent on frequency and the elastic modulus increases proportionally with fibrinogen concentration. Nevertheless, at high frequencies, G' increases with a slope of $\frac{1}{2}$ even after inertia corrections. Several studies have performed frequency sweeps to characterize the viscoelastic behavior of purified fibrin clots.[37,38] While not completely in accordance with our results, they show a purely elastic behavior since G' is much higher than G'' with a constant LVR without increment at high frequencies. To explain the differences in the viscoelastic

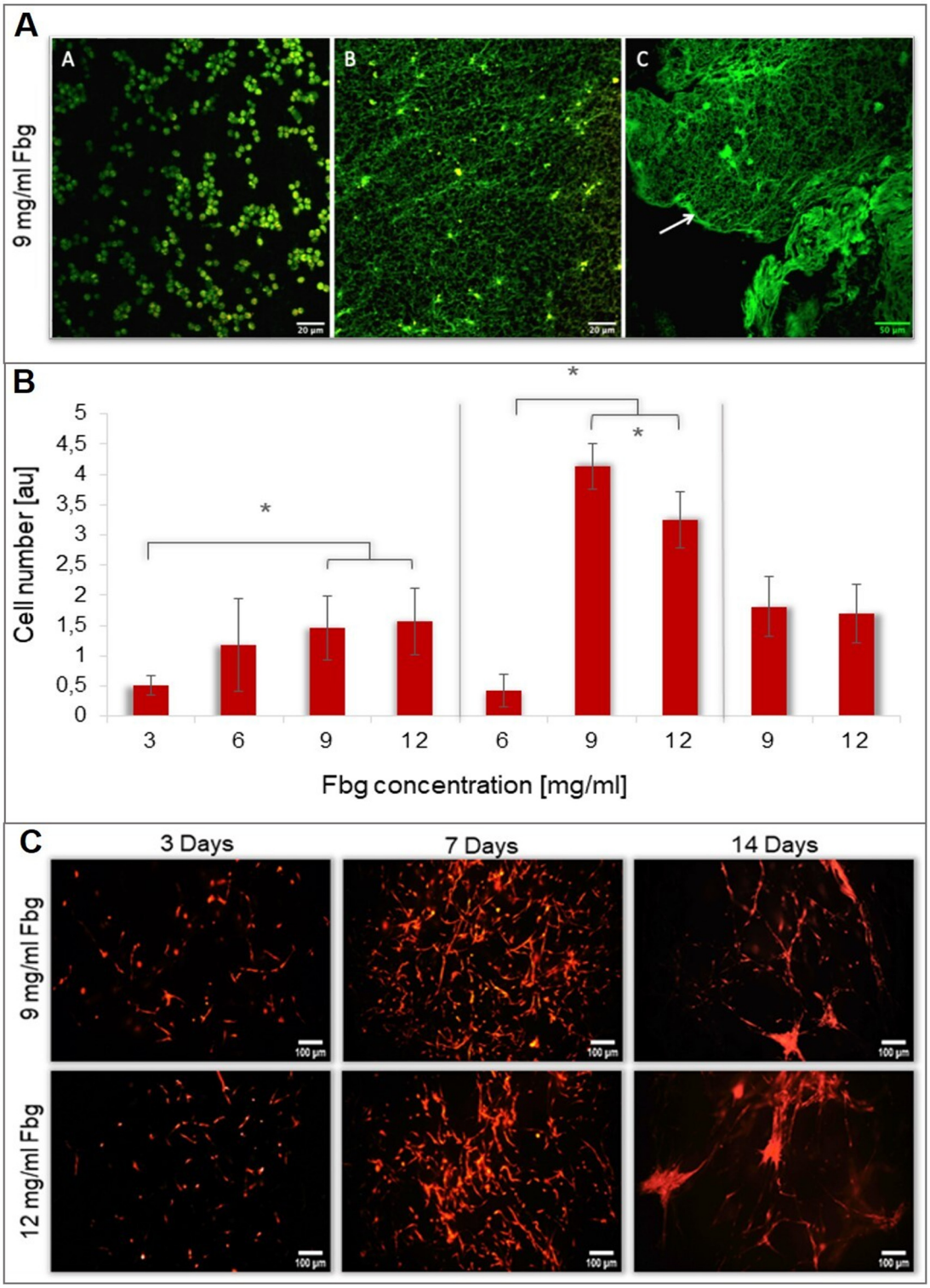

Fig. 4 MPM images of the Fbg–blood gel with 9 mg ml^{-1} fibrinogen: (A) 3 days of incubation; (B) 14 days of incubation and (C) 21 days of incubation. (B and C) DPC proliferation in Fbg–blood gels with different Fbg concentrations. On day 3, the values for 9 and 12 mg ml^{-1} Fbg are significantly higher than that for 3 mg ml^{-1}. On day 7, proliferation with 9 mg ml^{-1} Fbg is significantly higher ($p \leq 0.001$). On day 14, there is no significant difference.

behavior of the Fbg–blood gel at high frequencies, which differs from the classical purified fibrin gel, several factors should be considered.

First, the kinetics of fibrin polymerization could be diverse due to the different concentrations of molecules that interact, affecting the structure of fibrin clots and their mechanical

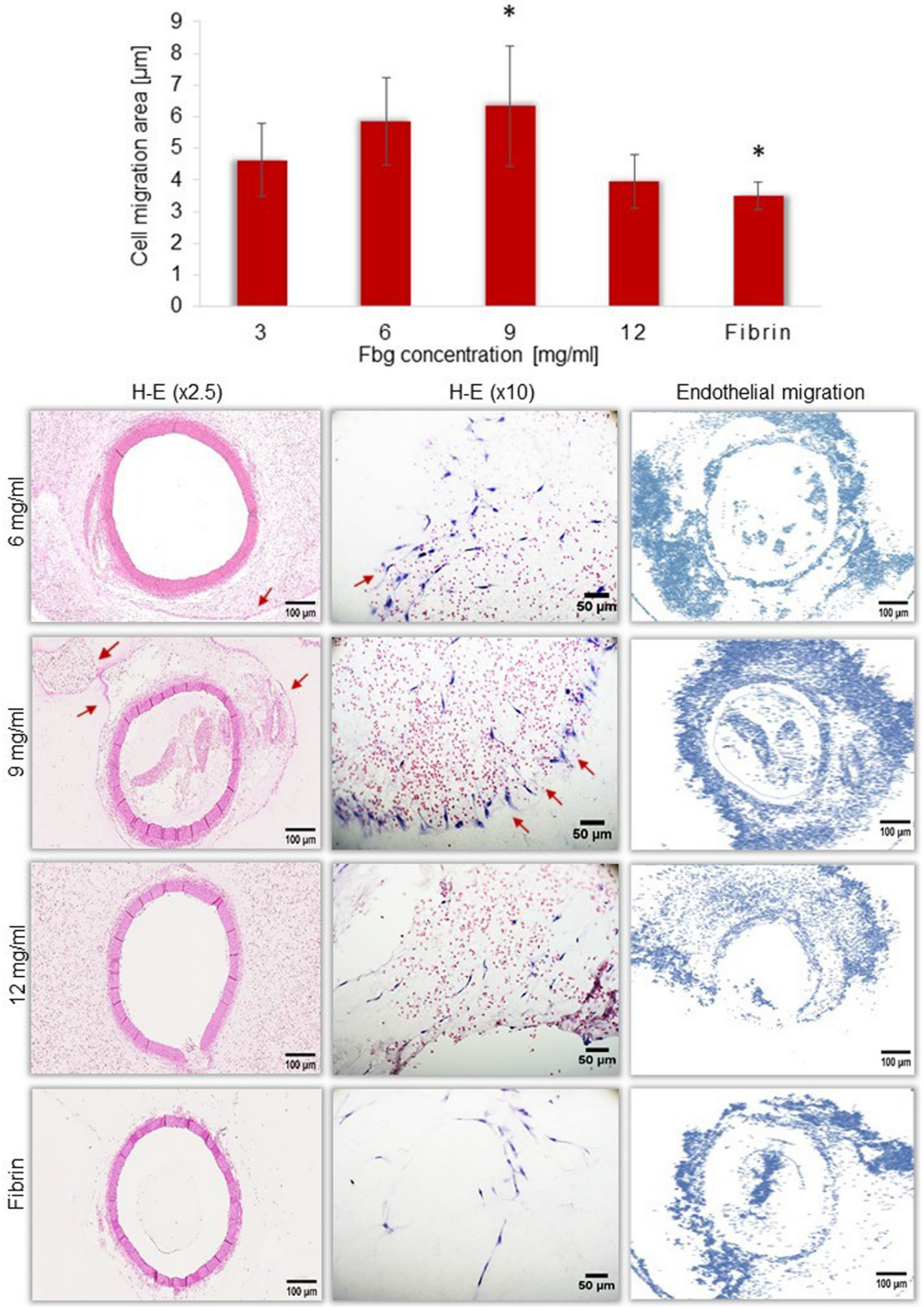

Fig. 5 Endothelial cell migration in the Fbg–blood gel – *ex vivo* aortic ring essay. Red arrows – the formation of tubule-like structure of endothelial cells.

properties.[39–41] For instance, variations in the fibrinogen/thrombin ratio affect the mechanical properties of fibrin. Previous studies performed on fibrin clots with a higher quantity of fibrinogen or a low quantity of thrombin suggest that an increased fibrinogen/thrombin ratio leads to coarser and thicker fibers with less lateral aggregation of protofibrils, making the clot more stiff, turbid, porous and permeable.[15,42] These clots reveal G' and G'' that increase with frequency.[36,43] Since the Fbg–blood gel has an increased fibrinogen/thrombin ratio (more Fbg and less thrombin) than a normal clot, G' and G'' are similar to those mentioned above, presenting thicker fibers, higher stiffness, and porosity.

Second, the presence of blood cells in the Fbg–blood gel has an impact on viscoelastic properties. In this regard, pre-

vious studies performed on gels obtained with purified fibrinogen and thrombin, without other blood components, affirmed that these clots differ from *in vivo* clots because cells and proteins present in plasma affect their structure and mechanical properties.[44] Few studies analyzed the mechanical properties of fibrin in clots by adding RBCs, proving that they modify the network's properties, resulting in coarser fibers with a larger pore size.[45,46]

Finally, the high molecular weight of fibrinogen molecules plays a key role in the mechanical properties of the clot. Fibrinogen is synthesized in a high molecular weight (HMW) form, but during polymerization, the αC region is degraded by thrombin resulting in two forms of Fbg with low molecular weight (LMW).[45] The αC region that remains intact in HMW Fbg determines the lateral aggregation of fibrin monomers, leading to coarse fibers.[47] As the Fbg–blood gel has a lower thrombin concentration, degradation of αC regions could be limited and its network should be mostly made of HMW Fbg.[46] This could explain the behavior of the Fbg–blood gel during frequency sweeps at high frequencies, exhibiting a slope of $\frac{1}{2}$ after inertia correction, which fits into the Rouse model for HMW polymers at high frequencies.[48]

Furthermore, requirements of an ideal biomaterial concern an adequate degradation rate that offers enough time for cells to secrete their matrix before the degradation of the scaffold. The degradation time of the Fbg–blood gel with 9 mg ml^{-1} Fbg and 50% blood could be in accordance with the extracellular matrix production rate.[49] Besides, hydrogels such as fibrin absorb liquids from the environment, interact with nutrients and deliver wastes. This ability is revealed by their swelling rate, which for the Fbg–blood gel is stable enough with 9 mg ml^{-1} Fbg and 50% of blood, allowing for molecular interchange without inducing considerable deformations in its structure. These results support the choice of the concentration of blood volume at 50% since the Fbg gel prepared with 80% blood shows a higher swelling rate that can be attributed to the greater abundance of red blood cells. These cells create a network with lower crosslink density, resulting in a more open structure that can swell more easily. Conversely, a hydrogel with a high degree of crosslinking will have a lower degree of swelling and be less flexible.[50] RBCs also affect the clot dissolution process,[51] explaining the faster degradation of the Fbg gel prepared with 3mg/ml Fbg and 80% blood. The higher presence of blood increases the quantity of components involved in fibrinolysis, such as Plasmin and Neutrophil.[43]

Another critical point for a successful scaffold is to ensure cell survival and proliferation.[9] Fibrin-based materials allow endothelial cell adhesion *via* integrin adhesion receptors and interactions with ECM proteins such as fibronectin and vitronectin.[52,53] Besides, the presence of these bioactive molecules within the scaffold enhances cell adhesion and survival.[10] The Fbg–blood gel has within its matrix bioactive molecules naturally present in blood platelets. Results show that the Fbg–blood gel allows cell survival and proliferation, and this is in accordance with previous studies conducted on fibrin-based preparations such as platelet-rich fibrin[54] and those proving cellular adhesion to fibrin.[52,53] Cell survival and proliferation in the Fbg–blood gel show a greater proliferation of DPCs with 9 mg ml^{-1} Fbg. After 14 days of incubation, cell organization into fibers and conglomerates can be observed.

This observation was confirmed by multiphoton microscopy. In the initial stages, no fiber networks were detected since fibrin did not produce a fluorescent signal after 2-PEF stimulation. After 2 weeks, a fluorescent organized network appears, suggesting the formation of an ECM composed of autofluorescent ECM proteins such as elastin, laminin, and proteoglycans.[55]

Finally, a successful scaffold should provide the neovessel formation. To evaluate the angiogenic potential of the Fbg–blood gel a rat aortic ring assay was proposed. This model has been used to study the angiogenic potential of biomaterials showing the development of microvascular networks as tubule-like structures in plasma clots, fibrin, collagen, and Matrigel.[56,57] After 10 days of aorta culture in the Fbg gel, histological analysis demonstrated that endothelial cell migration varies with changing Fbg concentration. Previous studies have shown that new capillary formation is higher at lower hydrogel stiffness and density.[58] These findings prompted the decision to test a higher range of Fbg concentrations, extending up to 12 mg ml^{-1} with the aim of obtaining more comprehensive results. Our findings proved that the Fbg–blood gel supports endothelial cell migration and capillary formation mostly with 9 mg ml^{-1} Fbg rather than with 12 mg ml^{-1} Fbg, confirming the validity of those previous studies.

Furthermore, angiogenic studies comparing the properties of fibrin networks built by HMW or LMW Fbg show that the fibrin matrix made by HMW Fbg develops coarse fibers with less lateral aggregation resulting in a porous and more permeable matrix that enhances the ingrowth of endothelial cells. This improvement of vessel-like structure formation in the porous network is explained by the ease of pericellular fibrin degradation by enzymes secreted by endothelial cells, which remodel the ECM and give place to cells to secrete a new ECM made of collagen and glycoproteins to form new capillaries.[43,59]

It is important to note that the components used in this laboratory study may differ from those used in the industrial product for regenerating dental pulp with the Fbg–blood gel. During clinical application, autologous blood is obtained by inducing periapical bleeding into the root canal and mixed with heterologous Fbg provided by authorized pharmaceutical industries authorized for human use. Although commercial Fbg can cause hypersensitivity, the low concentration and volume required for the final product significantly reduce the risk.

5. Conclusion

A method for constructing a dental pulp mimicking hydrogel using fibrinogen and human blood was developed. Evaluation

of the mechanical and biological properties of the Fbg–blood hydrogel reveals that this more rigid, porous, and permeable network could enhance angiogenesis and support the revascularization of the newly formed tissue. In addition, the survival and proliferation of dental pulp cells inside the gel could ensure the secretion of an extracellular matrix and the reorganization of a new pulp-like tissue. A further perspective before clinical application for RET is to apply the gel *in vitro* and *in vivo* inside the root canal. Besides, the versatility of the mechanical properties of this gel could pave the way for further applications in other regenerative medicine fields, for instance, smooth muscle or neuronal regeneration since these tissues possess a range of elasticity that could be mimicked by the Fbg–blood hydrogel.

Conflicts of interest

Authors disclose all conflicts of interest.

Acknowledgements

We acknowledge the rheological platform of LabEx NUMEV, Montpellier, France. We appreciate the technical support provided by M. Frédéric Guérin from the simulation platform, the Faculty of Medicine of Montpellier for obtaining animals for *ex vivo* studies and the Plateforme de Simulation "Réseau d'Histologie Expérimentale de Montpellier", RHEM, facility supported by SIRIC Montpellier Cancer Grant INCa_Inserm_DGOS_12553. We are grateful to the European Regional Development Foundation and the Occitanian Region (FEDER-FSE 2014-2020, Languedoc Roussillon), REACT-EU (Recovery Assistance for Cohesion and the Territories of Europe), IBiSA and Ligue contre le cancer for processing our animal tissues, performing histological techniques and sharing their expertise.

References

1 K. M. Fawzy El-Sayed, K. Jakusz, A. Jochens, C. Dörfer and F. Schwendicke, *Tissue Eng., Part B*, 2015, **21**, 451–460.
2 V. Orti, P.-Y. Collart-Dutilleul, S. Piglionico, O. Pall, F. Cuisinier and I. Panayotov, *Tissue Eng., Part B*, 2018, **24**, 419–442.
3 B.-N. Lee, J.-W. Moon, H.-S. Chang, I.-N. Hwang, W.-M. Oh and Y.-C. Hwang, *Restor. Dent. Endod.*, 2015, **40**, 179.
4 T. W. Lovelace, M. A. Henry, K. M. Hargreaves and A. Diogenes, *J. Endod.*, 2011, **37**, 133–138.
5 V. Chrepa, M. A. Henry, B. J. Daniel and A. Diogenes, *J. Dent. Res.*, 2015, **94**, 1653–1659.
6 A. S. Alobaid, L. M. Cortes, J. Lo, T. T. Nguyen, J. Albert, A. S. Abu-Melha, L. M. Lin and J. L. Gibbs, *J. Endod.*, 2014, **40**, 1063–1070.
7 O. Dianat, F. Mashhadi Abas, P. Paymanpour, M. J. Eghbal, S. Haddadpour and N. Bahrololumi, *Dent. Traumatol.*, 2017, **33**, 84–90.
8 M. C. Bottino, D. Pankajakshan and J. E. Nör, *Dent. Clin. North Am.*, 2017, **61**, 689–711.
9 F. J. O'Brien, *Mater. Today*, 2011, **14**, 88–95.
10 G. Raddall, I. Mello and B. M. Leung, *Front. Bioeng. Biotechnol.*, 2019, **7**, 317.
11 A. Riaz and F. A. Shah, *Tissue Eng. Regener. Med.*, 2021, **18**, 37–48.
12 E. Karsten, E. Breen and B. R. Herbert, *Sci. Rep.*, 2018, **8**, 3101.
13 V. Pretini, M. H. Koenen, L. Kaestner, M. H. A. M. Fens, R. M. Schiffelers, M. Bartels and R. Van Wijk, *Front. Physiol.*, 2019, **10**, 945.
14 P. de la Puente and D. Ludeña, *Exp. Cell Res.*, 2014, **322**, 1–11.
15 A. S. Wolberg, *Blood Rev.*, 2007, **21**, 131–142.
16 J. W. Weisel and R. I. Litvinov, *Subcell. Biochem.*, 2017, **82**, 405–456.
17 Y. Li, H. Meng, Y. Liu and B. P. Lee, *Sci. World J.*, 2015, **2015**, 1–10.
18 B. Chang, N. Ahuja, C. Ma and X. Liu, *Mater. Sci. Eng., R*, 2017, **111**, 1–26.
19 M. Ducret, A. Constantini, S. Gobert, J.-C. Farges and M. Bekhouche, *Eur: Cells Mater.*, 2021, **41**, 1–14.
20 L. Almany and D. Seliktar, *Biomaterials*, 2005, **26**, 2467–2477.
21 A. J. Man, H. E. Davis, A. Itoh, J. K. Leach and P. Bannerman, *Tissue Eng., Part A*, 2011, **17**, 2931–2942.
22 R. H. Ewoldt, M. T. Johnston and L. M. Caretta, in *Complex Fluids in Biological Systems*, ed. S. E. Spagnolie, Springer New York, New York, NY, 2015, pp. 207–241.
23 A. Franck, *Instrument Inertia Correction During Dynamic Mechanical Testing*, TA Instruments, 2005.
24 J. E. Sader, B. D. Hughes, J. A. Sanelli and E. J. Bieske, *Rev. Sci. Instrum.*, 2012, **83**, 055106.
25 H.-J. Butt, B. Cappella and M. Kappl, *Surf. Sci. Rep.*, 2005, **59**, 1–152.
26 M. Martin, O. Benzina, V. Szabo, A.-G. Végh, O. Lucas, T. Cloitre, F. Scamps and C. Gergely, *PLoS One*, 2013, **8**, e56286.
27 E. Hasanzadeh, S. Ebrahimi-Barough, E. Mirzaei, M. Azami, S. M. Tavangar, N. Mahmoodi, A. Basiri and J. Ai, *J. Biomed. Mater. Res., Part A*, 2019, **107**, 802–814.
28 P.-Y. Collart-Dutilleul, E. Secret, I. Panayotov, D. Deville de Périère, R. J. Martín-Palma, V. Torres-Costa, M. Martin, C. Gergely, J.-O. Durand, F. Cunin and F. J. Cuisinier, *ACS Appl. Mater. Interfaces*, 2014, **6**, 1719–1728.
29 J. Schindelin, I. Arganda-Carreras, E. Frise, V. Kaynig, M. Longair, T. Pietzsch, S. Preibisch, C. Rueden, S. Saalfeld, B. Schmid, J.-Y. Tinevez, D. J. White, V. Hartenstein, K. Eliceiri, P. Tomancak and A. Cardona, *Nat. Methods*, 2012, **9**, 676–682.
30 T. Cloitre, I. V. Panayotov, H. Tassery, C. Gergely, B. Levallois and F. J. G. Cuisinier, *J. Biophotonics*, 2013, **6**, 330–337.

31 M. Baker, S. D. Robinson, T. Lechertier, P. R. Barber, B. Tavora, G. D'Amico, D. T. Jones, B. Vojnovic and K. Hodivala-Dilke, *Nat. Protoc.*, 2012, **7**, 89–104.
32 Y. Song, J. Soto, B. Chen, L. Yang and S. Li, *Biomaterials*, 2020, **234**, 119743.
33 A. E. Stanton, X. Tong and F. Yang, *Acta Biomater.*, 2019, **96**, 310–320.
34 C. Erisken, D. M. Kalyon, J. Zhou, S. G. Kim and J. J. Mao, *J. Endod.*, 2015, **41**, 1711–1717.
35 P. Riha, X. Wang, R. Liao and J. F. Stoltz, *Clin. Hemorheol. Microcirc.*, 1999, **21**, 45–49.
36 K. Gersh, C. Nagaswami and J. Weisel, *Thromb. Haemostasis*, 2009, **102**, 1169–1175.
37 J. W. Weisel, *Biophys. Chem.*, 2004, **112**, 267–276.
38 J. M. Zuidema, C. J. Rivet, R. J. Gilbert and F. A. Morrison, *J. Biomed. Mater. Res., Part B*, 2014, **102**, 1063–1073.
39 R. R. Hantgan and J. Hermans, *J. Biol. Chem.*, 1979, **254**, 11272–11281.
40 J. W. Weisel and C. Nagaswami, *Biophys. J.*, 1992, **63**, 111–128.
41 R. I. Litvinov and J. W. Weisel, *Matrix Biol.*, 2017, **60–61**, 110–123.
42 B. Blombäck, D. Banerjee, K. Carlsson, A. Hamsten, B. Hessel, R. Procyk, A. Silveira and L. Zacharski, in *Fibrinogen, Thrombosis, Coagulation, and Fibrinolysis*, ed. C. Y. Liu and S. Chien, Springer US, Boston, MA, 1990, vol. 281, pp. 1–23.
43 N. Wohner, *Cardiovasc. Hematol. Agents Med. Chem.*, 2008, **6**, 224–228.
44 M. E. Carr and C. L. Hardin, *Am. J. Physiol.: Heart Circ. Physiol.*, 1987, **253**, H1069–H1073.
45 B. Holm, D. W. T. Nilsen, P. Kierulf and H. C. Godal, *Thromb. Res.*, 1985, **37**, 165–176.
46 B. Holm, F. Brosstad, P. Kierulf and H. C. Godal, *Thromb. Res.*, 1985, **39**, 595–606.
47 J. Z. Cui, A. Y. Tehrani, K. A. Jett, P. Bernatchez, C. van Breemen and M. Esfandiarei, *J. Struct. Biol.*, 2014, **187**, 242–253.
48 Y. Masubuchi, H. Takata, Y. Amamoto and T. Yamamoto, *Nihon Reoroji Gakkaishi*, 2018, **46**, 171–178.
49 O. Rosmark, E. Åhrman, C. Müller, L. Elowsson Rendin, L. Eriksson, A. Malmström, O. Hallgren, A.-K. Larsson-Callerfelt, G. Westergren-Thorsson and J. Malmström, *Sci. Rep.*, 2018, **8**, 5409.
50 F. Reyes Ortega, G. Rodríguez, M. Rosa Aguilar, J. García-Sanmartín, A. Martínez and J. San Román, *Biomecanica*, 2012, **20**, 7–19.
51 J. Weisel and R. Litvinov, *Cardiovasc. Hematol. Agents Med. Chem.*, 2008, **6**, 161–180.
52 M. Bacakova, J. Musilkova, T. Riedel, D. Stranska, E. Brynda, L. Bacakova and M. Zaloudkova, *Int. J. Nanomed.*, 2016, 771.
53 J. Ceccarelli and A. J. Putnam, *Acta Biomater.*, 2014, **10**, 1515–1523.
54 R. Khurana, P. Kudva and S. Husain, *J. Indian Soc. Periodontol.*, 2017, **21**, 16.
55 P. J. Campagnola and C.-Y. Dong, *Laser Photonics Rev.*, 2011, **5**, 13–26.
56 R. F. Nicosia, J. F. McCormick and J. Bielunas, *Scanning Electron Microsc.*, 1984, 793–799.
57 R. F. Nicosia and A. Ottinetti, *In Vitro Cell. Dev. Biol.*, 1990, **26**, 119–128.
58 S. M. Willerth, K. J. Arendas, D. I. Gottlieb and S. E. Sakiyama-Elbert, *Biomaterials*, 2006, **27**, 5990–6003.
59 E. A. Ryan, L. F. Mockros, J. W. Weisel and L. Lorand, *Biophys. J.*, 1999, **77**, 2813–2826.

